

Article

Extreme Droughts Change in the Mekong River Basin: A Multidisciplinary Analysis Based on Satellite Data

Vo Tuong ¹, Thanh-Van Hoang ^{2,*} , Tien-Yin Chou ² , Yao-Min Fang ², Chun-Tse Wang ², Thanh-Danh Tran ¹ 
and Dung Duc Tran ³ 

¹ Faculty of Civil Engineering, Ho Chi Minh City Open University, Ho Chi Minh City 700000, Vietnam; voquangtuong@gmail.com (V.T.); danh.tt@ou.edu.vn (T.-D.T.)

² Geographic Information System Research Center, Feng Chia University, 100 Wenhwa Rd., Situn, Taichung 40724, Taiwan; jimmy@gis.tw (T.-Y.C.); frankfang@gis.tw (Y.-M.F.); james@gis.tw (C.-T.W.)

³ Center of Water Management and Climate Change, Institute for Environment and Resources, Vietnam National University—Ho Chi Minh City (VNU-HCM), Ho Chi Minh City 700000, Vietnam; dungtranducvn@yahoo.com

* Correspondence: van@gis.tw

Abstract: This study evaluates droughts in the Mekong River Basin (MKB) based on a multidisciplinary method, mainly using the Standardized Precipitation Index (SPI) and Mann–Kendall (MK) test. Precipitation data corresponding to the seasonality of the regional climate were retrieved from Integrated Multi-satellitE Retrievals for Global Precipitation Measurement from 2001 to 2020, at a monthly temporal scale and 0.1 degree spatial resolution. Drought events and their average interval, duration, and severity were determined based on Run theory. Our results revealed the most extreme drought period was in January 2014, at the time the lowest precipitation occurred. Spatial extreme drought results indicated that Zone 2 in the upstream MKB has the highest frequency of drought, with 44 events observed during 19 years, and experiences the most severe droughts, whereas Zone 24 in the downstream MKB has the most prolonged drought duration of seven months. The periods and locations of extreme drought were identified using the SPI, corresponding to historic droughts of the MKB. Furthermore, the MK test shows an increasing trend of droughts in the lower MKB and the cluster analysis identified six clusters of times series. Overall, our study provides essential findings for international and national water resource stakeholders in identifying trends of extreme drought in the MKB.



Citation: Tuong, V.; Hoang, T.-V.; Chou, T.-Y.; Fang, Y.-M.; Wang, C.-T.; Tran, T.-D.; Tran, D.D. Extreme Droughts Change in the Mekong River Basin: A Multidisciplinary Analysis Based on Satellite Data. *Water* **2021**, *13*, 2682. <https://doi.org/10.3390/w13192682>

Academic Editor: Su-Chin Chen

Received: 3 September 2021

Accepted: 24 September 2021

Published: 28 September 2021

Publisher's Note: MDPI stays neutral with regard to jurisdictional claims in published maps and institutional affiliations.



Copyright: © 2021 by the authors. Licensee MDPI, Basel, Switzerland. This article is an open access article distributed under the terms and conditions of the Creative Commons Attribution (CC BY) license (<https://creativecommons.org/licenses/by/4.0/>).

Keywords: extreme drought; Mekong; SPI; Mann–Kendall; time series clustering; integrated multi-satellite retrievals (IMERG)

1. Introduction

Drought is among those natural disasters that have caused severe damage to humanity, society, economy, and environment [1–6]. In the three recent decades, droughts have occurred in many countries across the world, such as the United States [7], Brazil [8], China [9], and Vietnam [10]. Drought has affected the socio-economy by reducing crop productivity, cultivated area, and crop yield. As a result, drought has increased agricultural production costs and decreased the income of agricultural labor. Furthermore, the prices of food could be highly influenced by droughts. Severe drought can have complex effects, ranging beyond the direct impacts on crops and livestock to an array of indirect impacts associated with sanitation, nutrition, loss of livelihood, displaced populations, and international disputes [5].

The Mekong River flows through China, Myanmar, Thailand, Laos, Cambodia, and Vietnam and its catchment basin covers an area of 797,000 km² with more than 60 million people. The river begins in the Lasagongma Spring in the plateaus of Tibet and flows about 4350 km southeast to the East Sea of Vietnam. The Mekong River basin is divided

into two parts according to topography. The upstream is 1000 m above mean sea level, mainly in the south of China, and is the so-called upper part of the Mekong. The lower part, or the downstream, is less than 300 m compared to the mean sea level, extending from the south of Chinese-Lao border to Myanmar, Cambodia, and Vietnam. The average annual discharge of the Mekong River is about 15,000 km³/year. The Mekong is one of the most biologically diverse areas globally, with hundreds of types of fish and river dolphins, crocodiles, and otters. Fishing is an essential activity on the river. However, the Mekong River is also used extensively for navigation. According to statistics from the World Food Organization, more than 60% of the population in the region lives mainly on agriculture and fisheries and depends on hydroelectricity [11]. The climate of the Mekong River Basin (MKB) varies by topography, from a temperate seasonal climate in the upstream, to a tropical monsoon climate in the downstream area. The rainy season usually lasts from June to November, while the dry season usually lasts from December to May. The average annual rainfall of the MKB ranges from 600 to 1700 mm [12].

Along with economic development, increasing electricity demand has led to the construction of a series of hydroelectric projects in the upper Mekong. Consequently, there are noticeable changes in climate, soil, and the hydraulic regime of sediment in the area. Pokhrel et al. [12] reviewed studies on the effects of climate change, land-use change, hydropower dam construction, and hydrological regime on the Mekong River. The study emphasizes the need to consider human factors, climate change, hydrological regime, and farming factors and at the same time find solutions for sustainable development for the region. While seeking real solutions to solve the problems caused by upstream hydropower reservoirs, climate change, and agricultural changes, assessing rainfall distribution for the area is an urgent issue. A practical assessment and forecasting of rainfall distribution will help water resource managers to develop appropriate coping strategies and solutions for damage mitigation.

Due to the extensive study catchment, metering station data is often challenging to complete. The use of satellite imagery is suitable for rain assessment for the area. Nigam, Ruiz-Barradas, and Chafik [13] used satellite imagery developed by NASA and Japan, the Tropical Rainfall Measurement Mission (TRMM), to assess hydro-meteorological changes for the entire region. Wang et al. [14] used rainfall data taken from the Tropic Rainfall Measurement Mission (TRMM 3B42V7) satellite and monitoring station data from the Mekong River Commission to build a distributed hydrological model that aims to assess hydrological processes for the area. However, recent studies have shown rain data from the Integrated Multi-satellitE Retrievals (IMERG) satellite models are more accurate [14–18] than those taken from TRMM, CHIRPS, and PERSIANN-CCS satellites.

This study aims to address the abovementioned knowledge gap. We used IMERG satellite images taken during the past two decades (2001–2020) to evaluate the rainfall distribution for the entire MKB. We hypothesized that extreme droughts are increasing in many regions of the MKB. We tested our hypothesis using satellite data over the years 2001 to 2020. These data were analyzed based on the run theory and a multidisciplinary approach using the Standardized Precipitation Index (SPI), the Zonal Statistic Model, and the Mann–Kendal test. According to Wanders and Wada [19] and Dai, Zhao, and Chen [20], drought is impacted by climate change, which affects drought characteristics, including drought severity, drought duration, and drought area. The area affected by drought is large. Therefore, the observation is difficult to obtain with gauge measurement methods. Especially in developing countries, it is insufficient to investigate climatic environmental observations. This leads to the risk of uncertainty in predicting natural disasters such as drought. Therefore, our findings are valuable for supporting international and national water resource stakeholders in determining appropriate solutions for regional development in the MKB.

2. Data Availability and Methods

This study follows an integrated framework including the three main steps presented in Figure 1. In the first step, we created an automatic program to retrieve precipitation data from IMERG (retrieved from <https://gpm.nasa.gov/>, accessed date: 5 May 2021). The program requires determining the spatial coverages or areas of interest and the range of temporal interest or duration of data. It also requires a temporal interval step for data retrieval. In the second step, we computed the SPI for meteorological drought estimation. The last step is to extract the characteristics of drought corresponding to each eco-watershed of the Mekong River, using zonal statistics with drought properties determined by the run theory. After that, we estimated drought characteristics and drought trends to get the comprehensive drought properties by applying the Mann–Kendall test. In these steps, the extreme droughts based on time series clustering and the monthly drought trends detected by the Mann–Kendall test are the most important results.

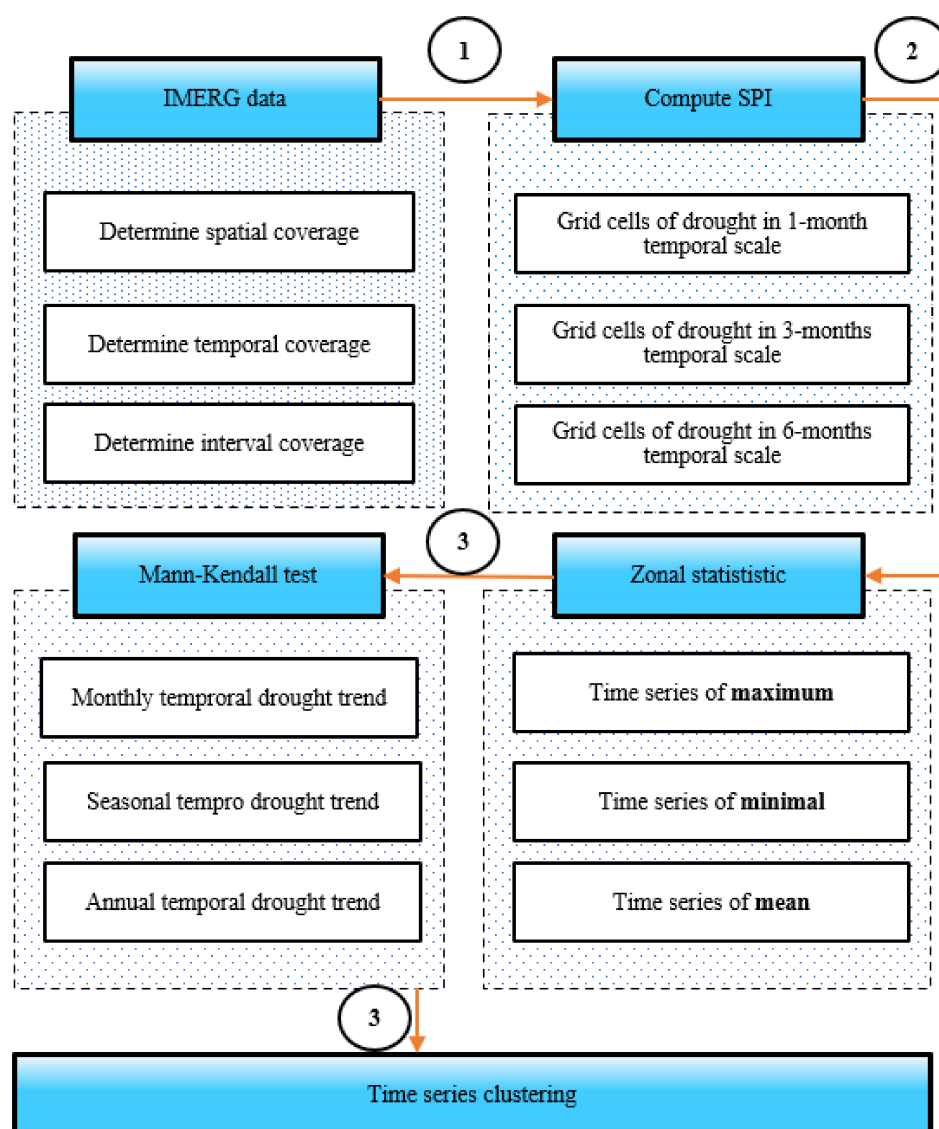


Figure 1. Methodology framework with the three main steps.

2.1. Study Area and Satellite Precipitation Data from IMERG

The study area covers the Mekong River Basin (MKB) with a latitude of 8.3–33.9 North and a longitude of 93.8–108.9 East (Figure 2). From its source on the Tibetan Plateau in China to the Mekong Delta, the main river goes throughout Myanmar, Thailand, Laos, Cambodia,

details the severe droughts in the downstream areas that cause heavy damage to crops, impacted the environment, and affected people's lives. In addition, the report also cites that the drought in 2016 caused severe economic losses in Thailand, estimated at \$1.7 billion US. The MKB has been at high risk of droughts and the increasing trend continues to exacerbate the risk, as evidenced by the increasing intensity and duration of the droughts that occurred in the past two decades. This is further confirmed by the findings of several climate change studies by the MRC and other organizations, showing the LMB is likely to see more severe droughts in the next 30 to 90 years due to less precipitation, high air temperatures, and high evapotranspiration combined with increasing demand for water as a result of the growing population in the basin.

In our study, monthly precipitation was retrieved from Integrated Multi-satellite Retrievals (IMERG). The IMERG products include early multi-satellite, late multi-satellite, and final satellite-gauge products with spatial and temporal resolutions of $1/10^\circ$ and 30 min. This system used the unified U.S.-developed algorithm that provides the day-1 multi-satellite precipitation product for the U.S. [22].

The study area was divided into 28 zones as ecology catchments and colored by the six MKB countries, following Gassert et al. [23]. We numbered zones following the latitude, identified from 1 to 28. Detailed zonal characteristics are described in Figure 2 and Table 1.

Table 1. Mekong zones classified by ecological characteristics by Gassert et al. [23].

Sub-Name	Main-Name	Country	Area (km ²)	Zonal ID
Za Qu	Mekong	China	45,083	1
Ngom Qu	Mekong	China	29,981	2
Qingshuilang Shah	Mekong	China	68,623	3
Weiyuan Jiang	Mekong	China	64,201	4
Nam Loi	Mekong	China	17,551	5
Nam Pho/Nam Ngaou	Mekong	Laos	12,481	6
Nam Mae Ing	Mekong	China	52,569	7
Nam Mae Kok	Mekong	Myanmar	16,654	8
Nam Beng/Nam Ngeun	Mekong	Laos	26,321	9
Nam Nhiep/Nam Sane	Mekong	Laos	12,759	10
Nam Beng/Nam Ngeun	Mekong	Laos	52,977	11
Nam Cadinh	Mekong	Laos	16,378	12
Songkhram	Mekong	Laos	16,513	13
Huai Luang/Nam Phoung/Nam	Mekong	Laos	9601	14
Nam Kam/Nam Hinboun/Huai	Mekong	Laos	11,708	15
Nam Kam/Nam Hinboun/Huai	Mekong	Laos	39,733	16
Nam Chi	Mekong	Thailand	53,461	17
Se Bang Nouan	Mekong	Cambodia	88,451	18
Se Kong	Mekong	Cambodia	50,831	19
Upper Tonle Sap	Mekong	Cambodia	49,903	20
Huai Tomo/Tonle Repon	Mekong	Cambodia	45,589	21
St. Sen	Mekong	Cambodia	29,546	22
Siem Bok	Mekong	Cambodia	41,001	23
Lagna Da Rgna	Viet Nam, Coast	Vietnam	9920	24
Dong Nai	Viet Nam, Coast	Cambodia	8746	25
Lagna Da Rgna	Viet Nam, Coast	Vietnam	42,359	26
Song Be Delta	Viet Nam, Coast	Vietnam	1873	27
Saigon	Viet Nam, Coast	Cambodia	74,097	28

2.2. Standardize Precipitation Index (SPI)

We calculated the Standardized Precipitation Index (SPI) using the methods derived from a concept by McKee et al. [24]. In this concept, drought is initiated by a decrease

in precipitation that causes a water shortage compared to water demand. The index is developed assuming that precipitation directly impacts hydrological variables (e.g., river discharge, groundwater, and soil moisture). The SPI has commonly been used to estimate the occurrence of meteorological drought due to its simplicity for calculation and applicability for various durations. The classification of drought levels based on the SPI referenced from Tsakiris and Vangelis [25] is presented in Table 2.

Table 2. Classification of SPI values.

Drought Category	Probability (%)	Values
Extreme wet	2.30	$2.00 \leq \text{SPI}$
Very wet	4.40	$1.99 \sim 1.50$
Moderately wet	9.20	$1.49 \sim 1.00$
Near normal	68.20	$0.99 \sim -0.99$
Moderate drought	9.20	$-1.00 \sim -1.49$
Severe drought	4.40	$-1.50 \sim -1.99$
Extreme drought	2.30	$-2.00 \geq \text{SPI}$

Source: Tsakiris and Vangelis (2004).

After computing several temporal scales, 1-month, 3-month, and 6-month, we proposed using 3 months (SPI3) as a typical drought index for later analyses.

2.3. Zonal Statistic Model

Zonal statistic methods were used to summarize and aggregate the raster values intersecting a vector geometry. For instance, zonal statistics provide the mean precipitation or maximum elevation of an administrative unit. Additionally, functions are provided to query a raster and get an interpolated value rather than the simple nearest pixel. The values within the zone were assumed to be normalized. The percentile was computed based on mean and standard deviation. For the extreme value of zone, the percentile method Q1 from Hyndman and Fan [26] was used for a query. The extreme drought values are determined when the non-linear integrated drought index (NDI) equals or is below the 10th percentile or corresponds to $z_{\text{score}} = -1.282$. The mean (μ), standard deviation (σ), z_{score} and percentile values of zone (x_p) were computed following Equations (1)–(4) below:

$$\mu = \frac{1}{N} \sum_i^N x_i \quad (1)$$

$$\sigma = \sqrt{\frac{1}{N} \sum_i^N (x_i - \mu)^2} \quad (2)$$

$$z_{\text{score}} = \frac{x - \mu}{\sigma} \quad (3)$$

$$x_p = z_{\text{score}} \times \sigma + \mu \quad (4)$$

In the next steps, the Mann–Kendall test, the empirical decomposition model, Moran's I statistic, and the G_i^* statistic are used to estimate tempo-spatial trends of extreme drought.

2.4. Drought Properties

Drought events and drought characteristics are determined using the run theory [27], presented in Figure 3. Drought events begin when the SPI value is lower than the threshold (-1 means moderate drought, and -2 means extreme drought) and continue until it is higher than the threshold. Drought severity (DS) is defined by the total value of the SPI [28]. Drought duration (DD) is defined by the number of months in the event [29]. Drought interval is the time between the beginning of a drought event and the beginning of the next drought event [30].

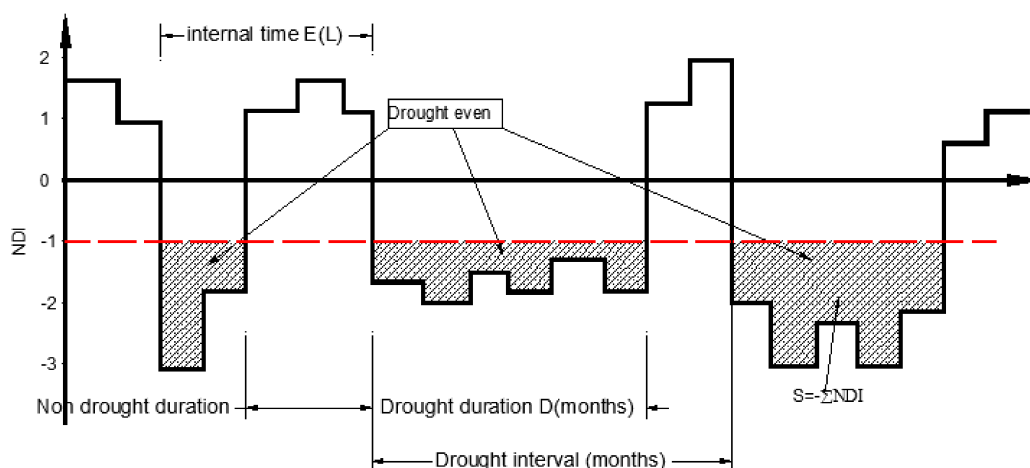


Figure 3. Drought characteristic based on the run theory.

2.5. Mann–Kendall Test

The Mann–Kendall test was used to detect the trends of historical droughts in the MKB. This method considers data distribution and can cope with outliers [31]. The processing of Mann–Kendall tests follows Equations (5) to (9) below:

$$Z_R = \frac{R - \frac{2N_1N_2}{N_1+N_2} + 1}{\sqrt{\frac{2N_1N_2(2N_1N_2 - N)}{N^2(N-1)}}} \tag{5}$$

where Z_R is run homogeneous test result, R is run number, N_1 is the number of values lower than median, and N_2 is the number of values higher than the median.

If Z_R value corresponds to 5% significance level or below, then the data is non-homogenous. Only homogeneous data are used to determine trend conditions [32].

The Mann–Kendall test is computed following Equations (6)–(9) below.

$$Z_{MK} = \begin{cases} \frac{S-1}{\sqrt{V(S)}} & \text{for } S > 0 \\ 0 & \text{for } S = 0 \\ \frac{S+1}{\sqrt{V(S)}} & \text{for } S < 0 \end{cases} \tag{6}$$

$$V(S) = \frac{n(n-1)(2n+5)}{18} \tag{7}$$

$$S = \sum_{k=1}^{n-1} \sum_{j=k+1}^n \text{sgn}(x_j - x_k) \tag{8}$$

$$\text{sgn}(x_j - x_k) = \begin{cases} +1 & \text{if } (x_j - x_k) > 0 \\ 0 & \text{if } (x_j - x_k) = 0 \\ -1 & \text{if } (x_j - x_k) < 0 \end{cases} \tag{9}$$

The Z_{MK} having a positive value means an increasing trend, a negative value means a decreasing trend, and a zero value means no trend. $V(S)$ is the variance and S is the Kendall sum statistic. The difference between each consecutive value is computed as positive (+1), negative (−1), and neural (0). x_j and x_k are value of time series at time j among n observational values. The trend is considered significant if Z_{MK} is higher than the significant levels. For instance, a confidence level of 90% has $\alpha = 10\%$ ($Z_{MK} \geq Z_{\alpha/2} = \pm 1.645$).

2.6. Time Series Clustering

We used K-Means and Hierarchical Clustering algorithms to group the dataset. K-Means clustering is a method that aims to partition n observations into k clusters. The cluster is built to follow the nearest mean (cluster centers or cluster centroid). K-Means clustering minimizes within-cluster variances (squared Euclidean distances). The term “K-Means” was first used in study [33]. The theory of the K-Means clustering method lets (Ω, A) be a probability space. Suppose we have a sequence of independent copies Z_1, Z_2, \dots, Z_n of random vector Z . The aim is to partition Ω into a finite number k of clusters $\Omega_1, \dots, \Omega_k$.

3. Results

3.1. Retrieved Precipitation IMERG Data

Based on the precipitation data retrieved from IMERG, we determined spatial distribution for precipitation in the MKB from 2001 to 2020 (Figure 4). Overall, the IMERG data performed well for the precipitation characteristics of the MKB, which were found to be similar compared with those from study [34]. The average monthly precipitation fluctuates in a range of lower than 10 mm to over 350 mm. Of those, the precipitation event in November 2014 had the lowest precipitation over the period, with the average monthly precipitation at 2.97 mm (Figure 4). The results also show that rainfall increases from January to August and decrease gradually from August to December. The most rainfall is in summer (JJA) and autumn (SON). Meanwhile, winter (DJF) and spring (MAM) rainfall are lower.

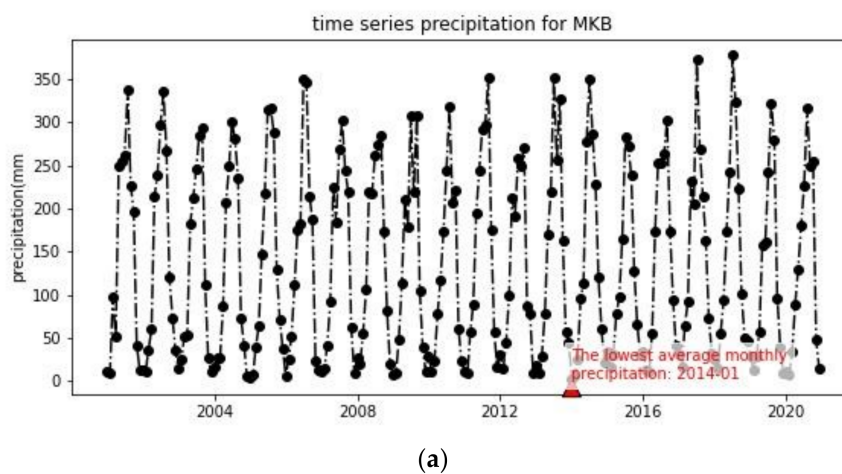


Figure 4. Cont.

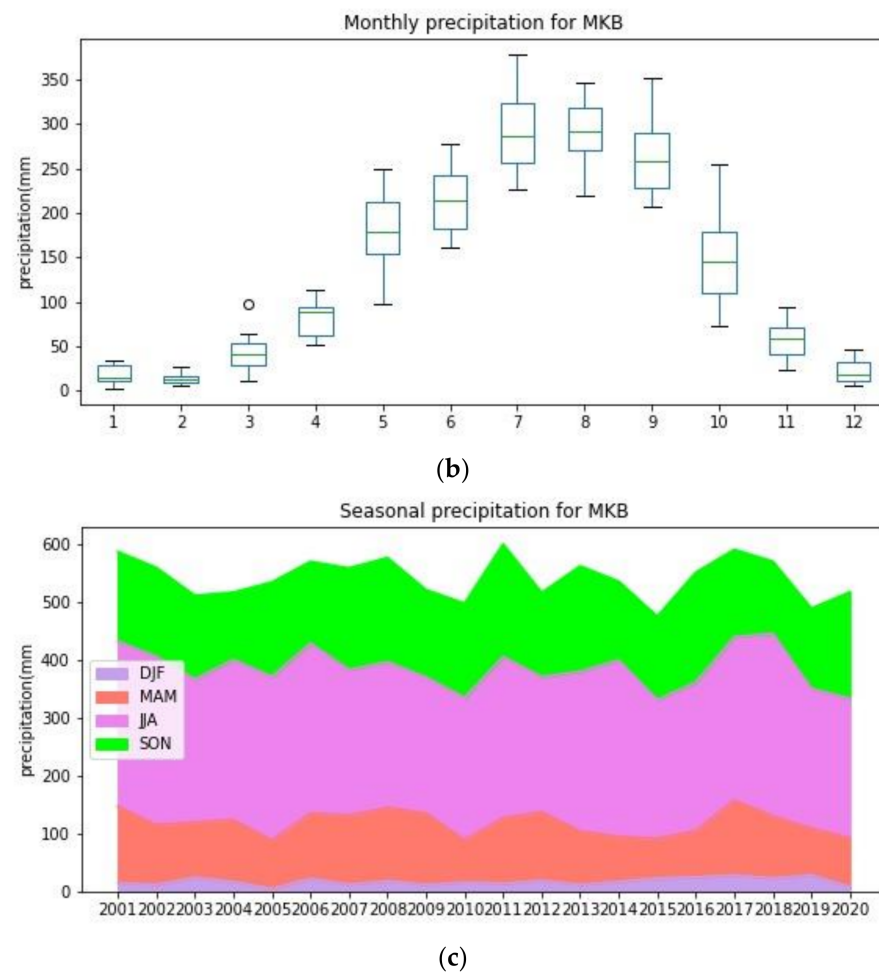


Figure 4. The lowest average monthly precipitation (a), monthly (b), and seasonal (c) precipitation of the MKB with DJF (December, January, February), MAM (March, April, May), JJA (June, July, August), and SON (September, October, November).

Rainfall in the MKB is not distributed differently between the upstream and downstream (Figure 5). However, in general, the climate in the MKB can be divided into two seasons: the rainy season and the dry season. The rainy season is from June to November, and the dry season is from November to May. This result is similar to the study by Lee and Dang [35]. Based on the analysis results, the IMERG satellite data were applied to the meteorological spatial analysis and spatial analysis for the MKB area.

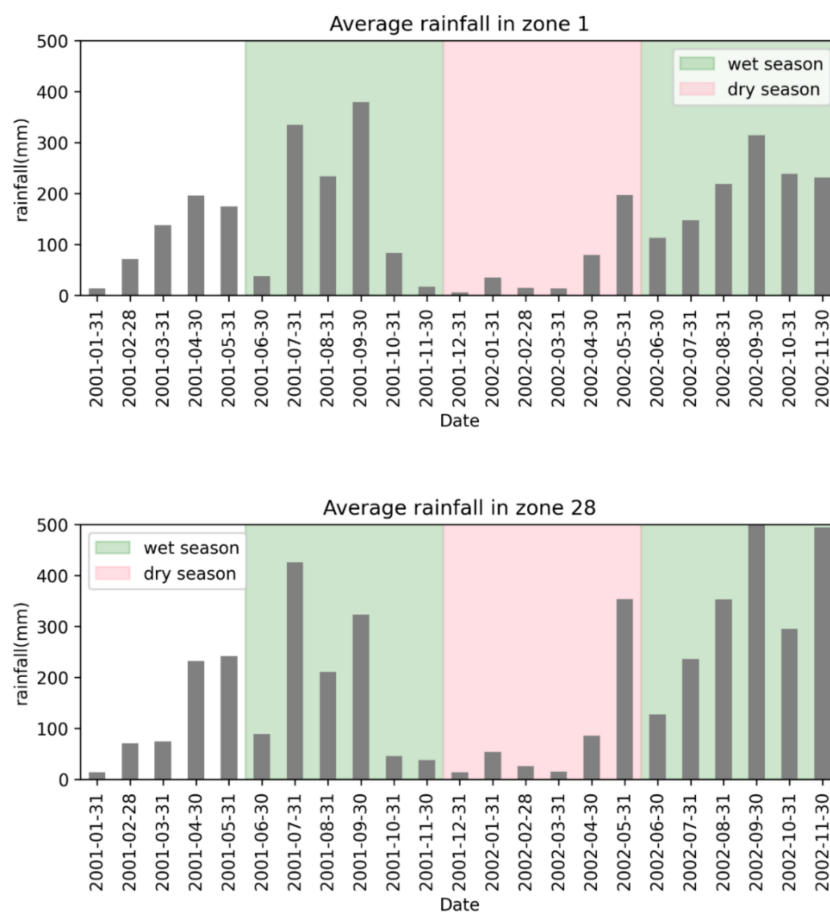


Figure 5. Average rainfall distribution in Zone 1 and Zone 28.

3.2. Simulation Results of Historical Droughts of the MKB Using SPI

To evaluate the spatial distribution of drought, we calculated the SPI index for the entire region before analyzing the max, min, mean, and standard derivation (std) values at each zone. Figure 6 shows the results of zonal statistical analysis in 2001–2002 with an example for Zone 1. Various raster pixel values of SPI in the same zone were compared using a zonal statistical model. Except for the std value, the max, min, and mean values tend to fluctuate quite similarly in Zone 1. Therefore, we chose the min value, because it is the one that causes the most extensive drought and poses the riskiest situation.

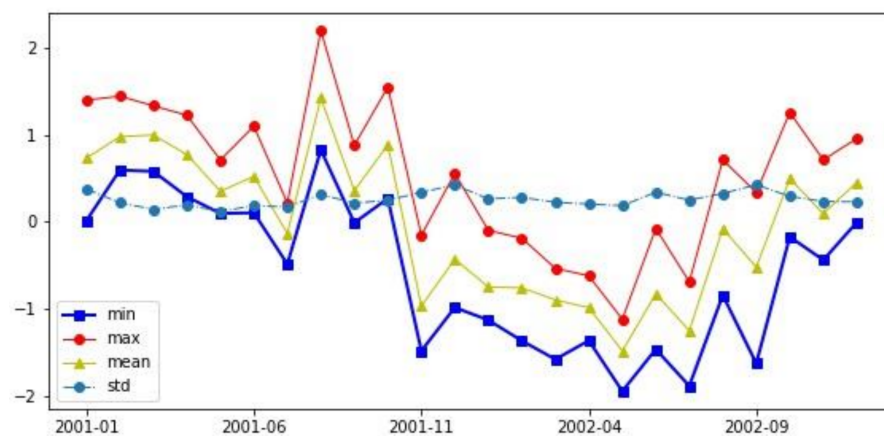


Figure 6. Zonal statistical calculations for Zone 1.

We computed the SPI to explore extreme drought severity events in the MKB. The analysis of historic drought determined that drought phenomena are complicated in the study area. The analysis results determined the spatial distribution and the dry time for the entire basin. The results show the differences in each zone’s drought characteristics, including the number of droughts that occurred, the duration, the severity, and the time interval between two consecutive droughts. According to the run theory, Zone 2 has the most frequent drought events (44 extreme drought events). Zone 26 has a minor drought, with eight extreme drought events (Figure 7). The circles in Figure 7’s graphs are the outliers that mainly occur when the drought duration in the region is more complex and unpredictable than the normal drought level. However, Zone 24 has the highest average drought duration of 7 months, while severe extreme droughts occurred under two months. The interval drought events, or the time between two drought events, indicate that the average interval of extreme drought is around ten months in the MKB.

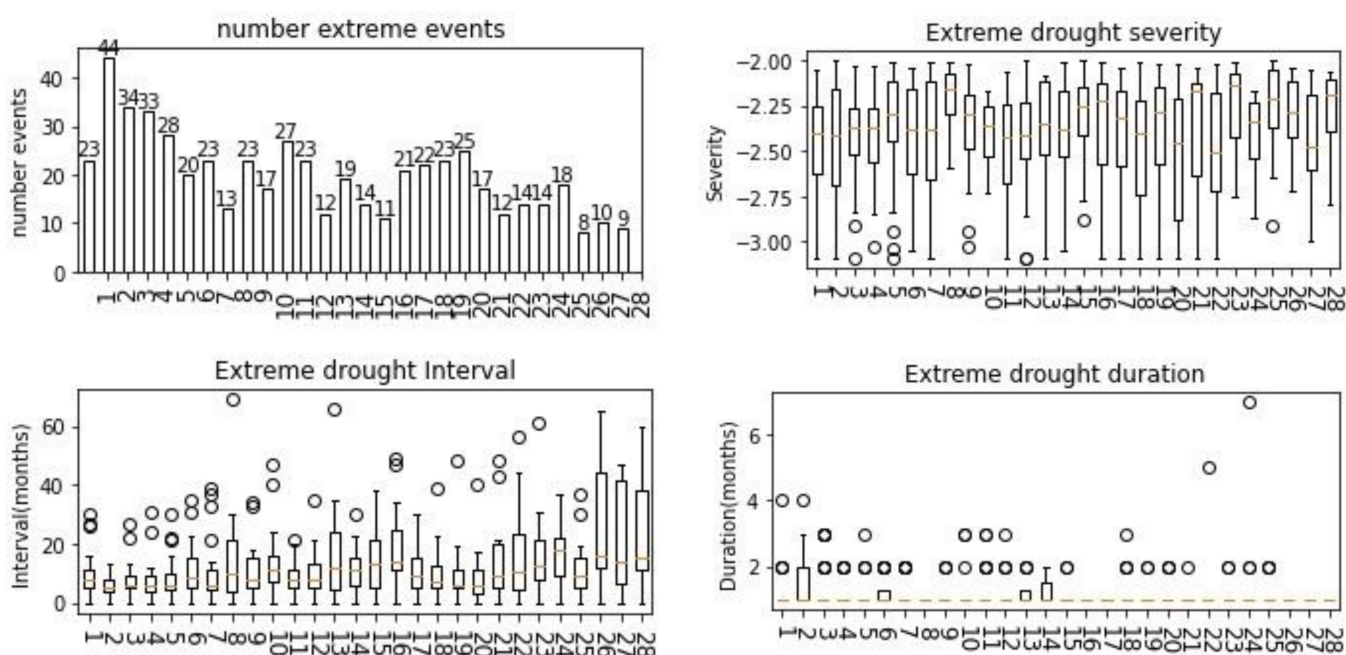


Figure 7. Extreme drought events, interval duration, drought severity, and drought duration for the MKB.

3.3. Trend of Extreme Drought Indicated by the Mann–Kendall Test

The Mann–Kendall test shows that the upper part of the MKB (Zones 1, 3, 4, 6, and 8) has increasing drought trends (Figure 8), while the lower part (Zones 5, 7, 9, 10–12, 14–16, 18–20, 23, 26, 27, and 28) has decreasing drought trends. The remaining zones have no significant drought trends, including the Mekong Delta in Cambodia and Vietnam.

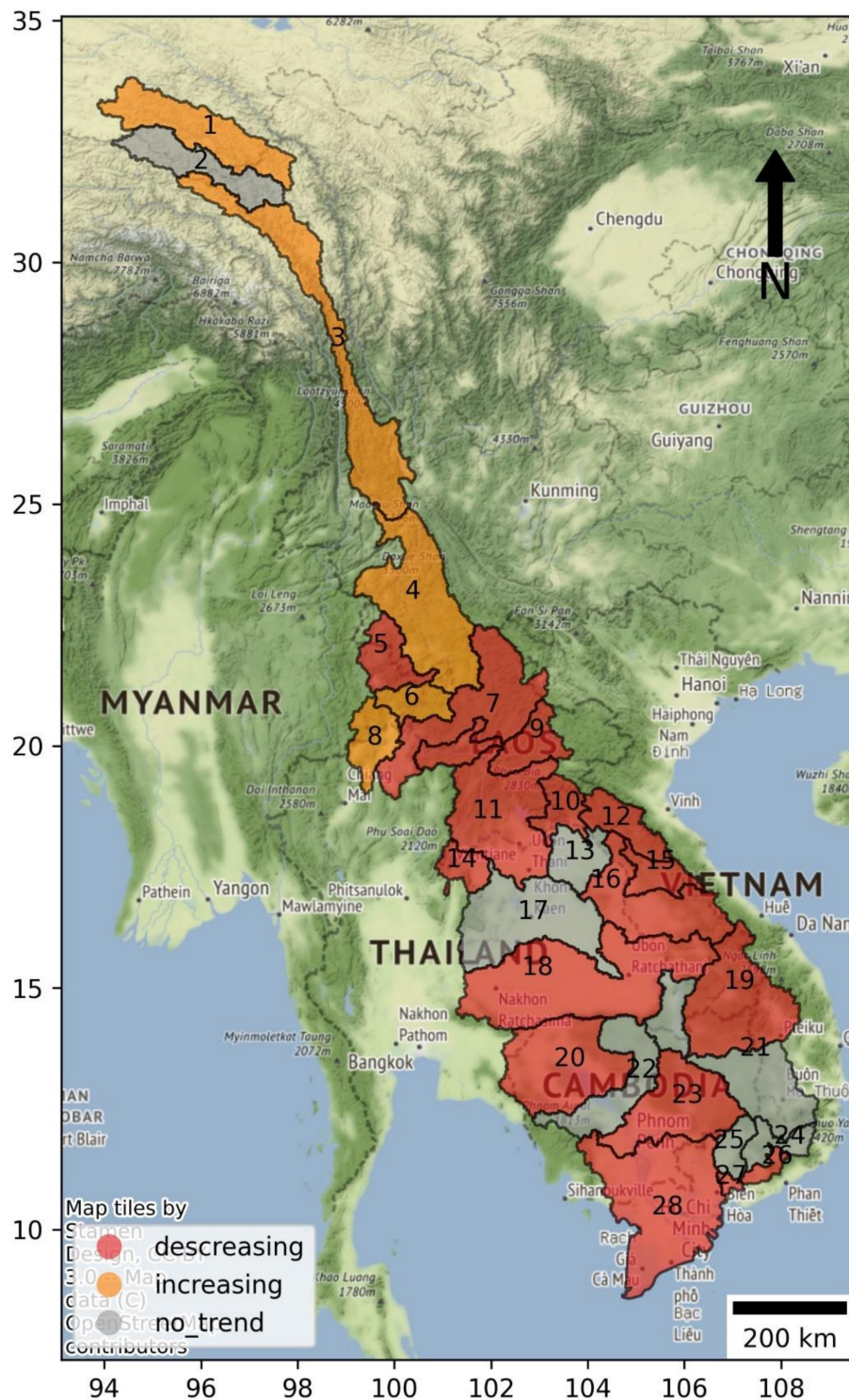


Figure 8. Trend of droughts in the MKB.

The results of the drought trend test show that most of the SPI indicators in the lower Mekong region tend to increase, or meteorological droughts have decreased. However, for a small area in the upper Mekong basin, SPI values decreased, or, in other words, meteorological drought increased (Figure 9). For example, Zone 1 in the upper Mekong tends towards increased drought (SPI decrease) with a rate of 0.002% in the past 20 years. Meanwhile, drought in the downstream area tends towards decrease (SPI increase) to a

similar degree. Details of MBK’s long-term trend analysis are presented in Table 3 and Figure 10 for slope changes in the zones.

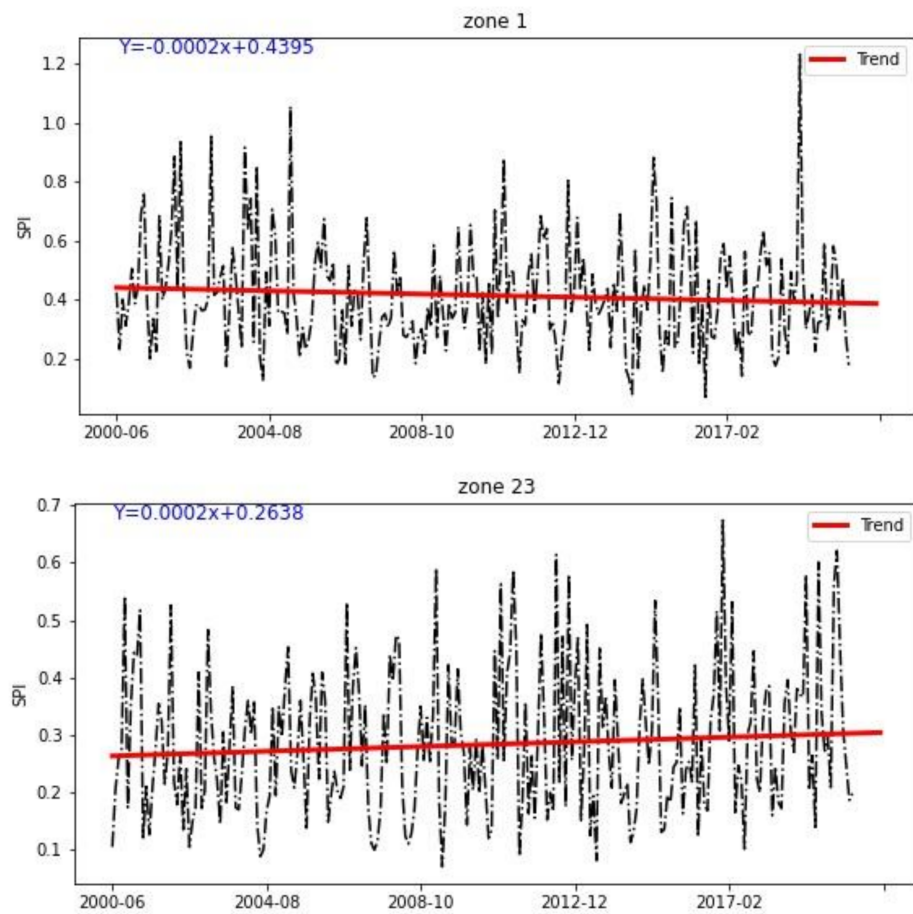


Figure 9. Trend of drought for Zone 1 and Zone 23 in the MKB.

Table 3. Drought trend and equation slopes of 28 zones within the MKB.

Zone	Trend	Equation	Zone	Trend	Equation
1	increasing	$Y = -0.0002x + 0.4395$	15	decreasing	$Y = 0.0002x + 0.2421$
2	no_trend	$Y = -0.0x + 0.6357$	16	decreasing	$Y = 0.0002x + 0.2486$
3	increasing	$Y = -0.0003x + 0.5832$	17	no_trend	$Y = 0.0x + 0.468$
4	increasing	$Y = -0.0002x + 0.5522$	18	decreasing	$Y = 0.0003x + 0.4116$
5	decreasing	$Y = 0.0002x + 0.3545$	19	decreasing	$Y = 0.0004x + 0.4464$
6	increasing	$Y = -0.0001x + 0.3857$	20	decreasing	$Y = 0.0004x + 0.4423$
7	decreasing	$Y = 0.0002x + 0.4203$	21	no_trend	$Y = -0.0x + 0.2823$
8	increasing	$Y = -0.0001x + 0.207$	22	no_trend	$Y = 0.0x + 0.2624$
9	decreasing	$Y = 0.0002x + 0.4526$	23	decreasing	$Y = 0.0002x + 0.2638$
10	decreasing	$Y = 0.0002x + 0.3552$	24	no_trend	$Y = 0.0x + 0.2664$
11	decreasing	$Y = 0.0004x + 0.46$	25	no_trend	$Y = 0.0x + 0.2834$
12	decreasing	$Y = 0.0002x + 0.381$	26	decreasing	$Y = 0.0001x + 0.123$
13	no_trend	$Y = 0.0x + 0.2479$	27	decreasing	$Y = 0.0001x + 0.276$
14	decreasing	$Y = 0.0001x + 0.3633$	28	decreasing	$Y = 0.0003x + 0.1946$

4. Discussion

4.1. Drought and Its Overall Impacts in the Mekong River Basin

This study has analyzed data retrieved from Integrated Multi-satellite Retrievals for Global Precipitation Measurement from 2001 to 2020. The analysis findings of the same seasonal pattern and the lowest precipitation occurred in November during the extreme drought event across the MKB countries. The most rainfall drops in summer (JJA) and autumn (SON), while winter (DJF) and spring (MAM) rainfall are lower. In addition, average monthly precipitation in the range of lower than 10 mm to over 350 mm in the period, and rainfall increases from January to August and gradual decreases from August to December, have implied that the data are reliable for applying SPI calculations and using the Mann–Kendall trend detection test [36–38].

The SPI calculations based on the run theory have revealed 44 extreme drought events as the most frequent occurrence in Zone 2 during the 19 analysis years. It means this zone (which belongs to China) should consider droughts in the coming years. This zone is located close to Zones 1, 3, and 4 (also belonging to China), which were detected as having increasing drought trends under the Man–Kendall test. Besides, the lowest extreme drought event (8 extreme events) was found in Zone 25 (which belongs to Cambodia) over the 19 years (Figure 7). Next to this zone, however, is Zone 24, which has the highest average drought duration of seven months compared to the remaining zones. Decreasing drought trends were found in Zones 5, 7, 9, 10–12, 14–16, 18–20, 23, 26, 27, and 28 in the lower part of the MKB (Myanmar, Thailand, Laos, Cambodia, Vietnam), which may indicate the increasing precipitation from 2001 to 2020, while the upper part (Zones 1, 3, 4, 6, and 8, located mainly in China) has increasing drought trends.

The Mann–Kendall test shows that the lower part of the MKB has decreasing drought trends, while the upper part has to deal with increasing drought trends. These results imply hydrological conditions of precipitation decreases downstream which are the same as those found by Dang et al. [39]. The remaining zones with no significant drought trends, such as those in the Mekong Delta (Cambodia and Vietnam) may be due to the relatively balanced water conditions in the area or insufficient data availability for the data we used for our analysis [35]. The results were also supported by the drought trend test, with increased SPI indicators found in the lower Mekong region, providing the decreasing trend of meteorological drought. However, our clustering results based on the K-Means Clustering method indicate that drought characteristics vary across the MKB, indicated by zone distributions; of those, only cluster 3 has all zones located in the lowest section at the same time. We realized that the meteorological limit is relatively uniform in the upper Mekong region, with slight fluctuation. Precipitation in the Mekong basin is subject to the precipitation oscillation explained by Räsänen and Kummu, (2013) [40]. However, the episodes of drought do not reveal any proven periodicity. This may explain the apparent low spatial coherence of the number of clusters, which may reflect local climatic conditions.

4.2. Policy Implication

The significant variability of precipitation across the zones of the countries in the MKB has been recognized in our study. Based on the findings, we recommend that countries with historical drought zones and those with increasing drought trends consider these phenomena in their water governance systems. These countries should enhance the capabilities developed for drought forecasting, warning, and preparedness systems. Although the member countries that belong to the MKB have long acknowledged the challenges associated with drought and natural disasters, the changing climate and other environmental pressures could exacerbate the phenomenon. Our study recommends developing a policy that focuses more on identifying solutions that minimize drought impact and exposure and maximize precipitation water storage for water use in the dry seasons.

4.3. Limitation and Future Outlook

Although this study has put great efforts into detecting drought trends in the MKB using various satellite image analysis methods, two main limitations are partially associated with the chosen method of calculating drought indexes for a large-scale area such as the MKB. First, the not-too-long period of observing satellite data (2001–2020) may partly influence the analysis results. This study uses statistical methods of analyzing satellite data, so the longer the time series data, the better the calculation to determine the extreme values. Second, the model could be improved if more observational data from the ground stations were available to adjust or assimilate into the models.

Based on the scope of this study, we only evaluated increasing and decreasing drought trends. Predicting the degree of increase and decrease of drought, such as intensity and time extreme, could be further studied. The Mann–Kendall test is a non-parametric method of trend assessment that does not consider serial correlation or seasonality effects. However, it is one of the simplest and most popular methods for analyzing and evaluating time-series-based trends. This study can be further extended using other trend analysis methods such as the Modified Mann–Kendall test [41], the Yue and Wang Modified M–K Test [36], or the Seasonal Sen’s Slope Estimator [41] to calculate serial autocorrelation and seasonality.

5. Conclusions

In this study, a multidisciplinary analysis based on satellite data is used to detect droughts and their trends in the Mekong River Basin (MKB) regarding how their historical dynamics could be explained for seeking potential adaptation and mitigation measures in the coming years. To our knowledge, this is one of the first studies integrating IMERG satellite images analyzed by various methods. In this study, we have therefore shown the trajectory of drought dynamics, the highest and lowest frequent droughts, and the locations and durations of droughts across the MKB. We argue that the method used by this study has broad transferability, offering the potential for drought assessments in regions worldwide facing similarly intense changes, particularly in the context of climate change.

The findings of this study reveal that even rainfall data are sufficient for drought detections, and that these types of data, particularly in terms of satellite images, present a dynamic drought process across the MKB. First, the zones with high rainfall in the upper basin show decreasing drought trends, which are not the same for those in downstream areas. Second, it should be noted that the lowest and highest severe droughts changed across the river basin with different durations, implying that future drought trends are complex. These would be indicators of a movement towards unsustainability, which should be taken into account by the countries in the MKB.

Author Contributions: V.T. developed the methodology and concept, performed data analysis and structured and wrote the first draft; T.-V.H. and D.D.T. reviewed literature, wrote the draft version, edited the manuscript and hydrographs, and managed correspondence; T.-D.T. and C.-T.W. analyzed data and provided maps, T.-Y.C. and Y.-M.F. reviewed the state-of-the-art and supervised the team. All authors have read and agreed to the published version of the manuscript.

Funding: This work was funded by Ho Chi Minh City Open University under grant number E2020.05.01.

Institutional Review Board Statement: Not applicable.

Informed Consent Statement: Not applicable.

Data Availability Statement: Not applicable.

Acknowledgments: This work was funded by Ho Chi Minh City Open University under grant number E2020.05.01. We also thank the Geographic Information Research Center—Feng Chia University Taiwan for their valuable comments and support.

Conflicts of Interest: The authors confirm that there is no conflict of interest.

References

1. Nguyen, N.A. Historic drought and salinity intrusion in the Mekong Delta in 2016: Lessons learned and response solutions. *Vietnam J. Sci. Technol. Eng.* **2017**, *59*, 93–96. [CrossRef]
2. Development, M. of A. and R. *The Drought and Saltwater Intrusion in the Highlands, South Middle Region, and Vietnamese Mekong Delta in 2016 and Proposed Actions 2016*. Available online: <https://reliefweb.int/report/viet-nam/vietnam-drought-and-saltwater-intrusion-emergency-plan-action-epoa-dref-operation-n> (accessed on 3 March 2021).
3. Thao, N.T.T.; Khoi, D.N.; Xuan, T.T.; Tychon, B. Assessment of Livelihood Vulnerability to Drought: A Case Study in Dak Nong Province, Vietnam. *Int. J. Disaster Risk Sci.* **2019**, *10*, 604–615. [CrossRef]
4. Ahmadalipour, A.; Moradkhani, H. Multi-dimensional assessment of drought vulnerability in Africa: 1960–2100. *Sci. Total Environ.* **2018**, *644*, 520–535. [CrossRef]
5. Barlow, M.; Zaitchik, B.; Paz, S.; Black, E.; Evans, J.; Hoell, A. A Review of Drought in the Middle East and Southwest Asia. *J. Clim.* **2016**, *29*, 8547–8574. [CrossRef]
6. Tre, B.; Vinh, T.; Giang, K. *Vietnam. The Drought and Salinity Intrusion in the Mekong River Delta of Vietnam*; CGIAR Research Centers in Southeast Asia Centers: Gelderland, The Netherlands, 2016.
7. Alexander, L. V Global observed long-term changes in temperature and precipitation extremes: A review of progress and limitations in IPCC assessments and beyond. *Weather Clim. Extrem.* **2016**, *11*, 4–16. [CrossRef]
8. Ribeiro, I.O.; Andreoli, R.V.; Kayano, M.T.; Sousa, T.R.; Medeiros, A.S.; Godoi, R.H.M.; Godoi, A.F.L.; Junior, S.D.; Martin, S.T.; Souza, R.A.F. Biomass burning and carbon monoxide patterns in Brazil during the extreme drought years of 2005, 2010, and 2015. *Environ. Pollut.* **2018**, *243*, 1008–1014. [CrossRef] [PubMed]
9. Pescaroli, G.; Alexander, D. Understanding Compound, Interconnected, Interacting, and Cascading Risks: A Holistic Framework. *Risk Anal.* **2018**, *38*, 2245–2257. [CrossRef] [PubMed]
10. Le, P.V.V.; Phan-Van, T.; Mai, K.V.; Tran, D.Q. Space-time variability of drought over Vietnam. *Int. J. Climatol.* **2019**, *39*, 5437–5451. [CrossRef]
11. Frenken, K. Irrigation in Central Asia in Figures: AQUASTAT Survey-2012. *FAO Water Rep.* **2013**, *39*, 1020–1203.
12. Pokhrel, Y.; Burbano, M.; Roush, J.; Kang, H.; Sridhar, V.; Hyndman, D.W. A review of the integrated effects of changing climate, land use, and dams on Mekong river hydrology. *Water* **2018**, *10*, 266. [CrossRef]
13. Nigam, S.; Ruiz-Barradas, A.; Chafik, L. Gulf Stream excursions and sectional detachments generate the decadal pulses in the Atlantic multidecadal oscillation. *J. Clim.* **2018**, *31*, 2853–2870. [CrossRef]
14. Wang, W.; Lu, H.; Yang, D.; Sothea, K.; Jiao, Y.; Gao, B.; Peng, X.; Pang, Z. Modelling hydrologic processes in the Mekong River Basin using a distributed model driven by satellite precipitation and rain gauge observations. *PLoS ONE* **2016**, *11*, e0152229. [CrossRef]
15. Fang, J.; Yang, W.; Luan, Y.; Du, J.; Lin, A.; Zhao, L. Evaluation of the TRMM 3B42 and GPM IMERG products for extreme precipitation analysis over China. *Atmos. Res.* **2019**, *223*, 24–38. [CrossRef]
16. Zhang, Z.; Tian, J.; Huang, Y.; Chen, X.; Chen, S.; Duan, Z. Hydrologic evaluation of TRMM and GPM IMERG satellite-based precipitation in a humid basin of China. *Remote Sens.* **2019**, *11*, 431. [CrossRef]
17. Ma, Q.; Li, Y.; Feng, H.; Yu, Q.; Zou, Y.; Liu, F.; Pulatov, B. Performance evaluation and correction of precipitation data using the 20-year IMERG and TMPA precipitation products in diverse subregions of China. *Atmos. Res.* **2020**, *249*, 105304. [CrossRef]
18. Jiang, S.; Wei, L.; Ren, L.; Xu, C.-Y.; Zhong, F.; Wang, M.; Zhang, L.; Yuan, F.; Liu, Y. Utility of integrated IMERG precipitation and GLEAM potential evapotranspiration products for drought monitoring over mainland China. *Atmos. Res.* **2020**, *247*, 105141. [CrossRef]
19. Wanders, N.; Wada, Y. Human and climate impacts on the 21st century hydrological drought. *J. Hydrol.* **2015**, *526*, 208–220. [CrossRef]
20. Dai, A.; Zhao, T.; Chen, J. Climate change and drought: A precipitation and evaporation perspective. *Curr. Clim. Chang. Rep.* **2018**, *4*, 301–312. [CrossRef]
21. Mekong River Commission, M. Annual Report: 2019. Available online: <http://interactive.mrcmekong.org/mrc-annual-report-2019/homepage/> (accessed on 23 September 2021).
22. Gan, F.; Gao, Y.; Xiao, L. Comprehensive validation of the latest IMERG V06 precipitation estimates over a basin coupled with coastal locations, tropical climate and hill-karst combined landform. *Atmos. Res.* **2021**, *249*, 105293. [CrossRef]
23. Gassert, F.; Rai, P.; Reig, P.; Luck, M. Mekong river basin study. *World Resour. Inst. Work. Pap.* **2012**. Available online: <https://www.wri.org/data/mekong-river-basin-study> (accessed on 23 September 2021).
24. McKee, T.B.; Doesken, N.J.; Kleist, J. The relationship of drought frequency and duration to time scales. In Proceedings of the 8th Conference on Applied Climatology, Anaheim, CA, USA, 17–22 January 1993; Volume 17, pp. 179–183.
25. Tsakiris, G.; Vangelis, H. Towards a Drought Watch System based on Spatial SPI. *Water Resour. Manag.* **2004**, *18*, 1–12. [CrossRef]
26. Hyndman, R.J.; Fan, Y. Sample quantiles in statistical packages. *Am. Stat.* **1996**, *50*, 361–365.
27. Guerrero-Salazar, P.L.A.; Yevjevich, V.M. Analysis of Drought Characteristics by the Theory of Runs. Ph.D. Thesis, Colorado State University, Libraries, Fort Collins, CO, USA, 1975.
28. Wu, R.; Zhang, J.; Bao, Y.; Guo, E. Run Theory and Copula-Based Drought Risk Analysis for Songnen Grassland in Northeastern China. *Sustainability* **2019**, *11*, 6032. [CrossRef]

29. Montaseri, M.; Amirataee, B.; Nawaz, R. A Monte Carlo Simulation-Based Approach to Evaluate the Performance of three Meteorological Drought Indices in Northwest of Iran. *Water Resour. Manag.* **2017**, *31*, 1323–1342. [[CrossRef](#)]
30. Ayantobo, O.O.; Li, Y.; Song, S. Multivariate Drought Frequency Analysis using Four-Variate Symmetric and Asymmetric Archimedean Copula Functions. *Water Resour. Manag.* **2019**, *33*, 103–127. [[CrossRef](#)]
31. Ali, R.; Kuriqi, A.; Abubaker, S.; Kisi, O. Long-Term Trends and Seasonality Detection of the Observed Flow in Yangtze River Using Mann-Kendall and Sen's Innovative Trend Method. *Water* **2019**, *11*, 1855. [[CrossRef](#)]
32. Güçlü, Y.S. Improved visualization for trend analysis by comparing with classical Mann-Kendall test and ITA. *J. Hydrol.* **2020**, *584*, 124674. [[CrossRef](#)]
33. MacQueen, J. Some methods for classification and analysis of multivariate observations. In Proceedings of the Fifth Berkeley Symposium on Mathematical Statistics and Probability, Oakland, CA, USA, 1 January 1967; Volume 1, pp. 281–297.
34. Thilakarathne, M.; Sridhar, V. Characterization of future drought conditions in the Lower Mekong River Basin. *Weather Clim. Extrem.* **2017**, *17*, 47–58. [[CrossRef](#)]
35. Lee, S.K.; Dang, T.A. Spatio-temporal variations in meteorology drought over the Mekong River Delta of Vietnam in the recent decades. *Paddy Water Environ.* **2019**, *17*, 35–44. [[CrossRef](#)]
36. Yue, S.; Wang, C. The Mann-Kendall Test Modified by Effective Sample Size to Detect Trend in Serially Correlated Hydrological Series. *Water Resour. Manag.* **2004**, *18*, 201–218. [[CrossRef](#)]
37. Hundertmark, W. Building drought management capacity in the Mekong River basin. *Irrig. Drain.* **2008**, *57*, 279–287. [[CrossRef](#)]
38. Dang, V.H.; Tran, D.D.; Cham, D.D.; Hang, P.T.; Nguyen, H.T.; Truong, H.V.; Tran, P.H.; Duong, M.B.; Nguyen, N.T.; Le, K.V.; et al. Assessment of Rainfall Distributions and Characteristics in Coastal Provinces of the Vietnamese Mekong Delta under Climate Change and ENSO Processes. *Water* **2020**, *12*, 1555. [[CrossRef](#)]
39. Räsänen, T.; Kumm, M. Spatiotemporal influences of ENSO on precipitation and flood pulse in the Mekong River Basin. *J. Hydrol.* **2013**, *476*, 154–168. [[CrossRef](#)]
40. Hamed, K.H.; Ramachandra Rao, A. A modified Mann-Kendall trend test for autocorrelated data. *J. Hydrol.* **1998**, *204*, 182–196. [[CrossRef](#)]
41. Hipel, K.W.; McLeod, A.I. (Eds.) Chapter 23 Nonparametric Tests for Trend Detection. In *Time Series Modelling of Water Resources and Environmental Systems*; Elsevier: Amsterdam, The Netherlands, 1994; Volume 45, pp. 853–938. ISBN 0167-5648.